Contents

List of Figures

List of Tables

Acknowledgements

I would like to express my sincere gratitude to Professors Dr. José Miguel da Silva, Dr. Pedro Viera Gamboa for their academic supervision, support and kind encouragement throughout the work period in Universiade da Beira Interior.

To Professors Dr. Ricardo Claudio and Dr. Nuno Nunes of Instituto Politécnico de Setúbal for their help, wise advice and logistical support for my stay in Setúbal during the laboratory test.

To professor Dr. Abilio Silva for his suggestions and willingness to my queries in the laboratory.

I would like to thank all those teachers of ETSIA who have been an example for me and for those who feel a special admiration, specially professors Dr. Gomez Tierno, Dr.Lola Sondesa, Dr. Bartolo Luque, Dr. Victoria Lapuerta, Dr. Pablo Rodríguez and Dr. J. Sagredo.

I want to express my gratitude to my Portuguese mates in the UBI for their generous and important support. Especially to João, Filipe, Marcio, Sara

Neither I can forget the staff of Extension Universitaria y Relaciones Internacionales of ETSIA that will always keep a nice memory for the time that i was there. Thank you very much to Aurora,Deli, Mercedes and Vicky.

Dedicated to my friends of the ETSIA.

Finally and not less important I want to be grateful for the support of my parents, my grandparents and my brother since without them this would not be possible.

Abstract

In general it is very important to know the dynamic response of any structure submitted to loads and based on it to modify it mass, stiffness, or damping properties of the same one finally to obtain a desired response within a margins of safety considering the life of the structure.

The damping properties of the structure were modified trough the use a passive damping to control the vibrations in structure with energy saving benefits with regard to the active control and also for its facility of implementation reducing the probability of failure of the system.

In the context of passive damping a variation of the loss factor was achieved based on the introduction of a viscoelastic material in a CFRP laminate structure by experimental tests using by bandwidth method.

Cork was used as a viscoelastic material for its lightness and low relative price and showing a great potential in the aeronautical field for vibration control in a high number of aeroelastic phenomena. The use of cork based composites can also be thought in space components in the form of sandwiches with cork cores or high performance fiber reinforced composites with embedded cork dust aiming at minimizing the vibration occurrence of large structures, which must have high stability requirements in terms of displacement and rapid damping vibrations caused by any disturbance in the system.

One most ambitious application of cork based composites refers to the structure of solar sails. This type of spacecraft only needs large sails and deployable booms that keep the sails deployed and support the the transmitted loads. Thus the study of the loads and vibrations that affect the booms is very important.

In the present case a passive damping using a design that comprises a viscoelastic material sandwiched between multiple CFRP layers was considered

envisaging decreasing the amplitude of the vibrations in the boom induced by the operation of the AOCS.

A computational analysis of this configuration of the material was developed using a finite element model (FEM) code to obtain the main dynamic properties of the structure, such as the natural frequencies and loss factors. Numerical results were validated through the comparison with the dynamic response of the material as obtained in experimental testing. Moreover, the improved damping properties found on cork based materials allow concluding that this type of viscoelastic material is a viable passive solution for vibration control with minimum penalties in the final weight of the structure.

List of symbols

α	mass proportional damping factor
β	stiffness proportional damping factor
$[F]$	damping matrix of the system
$[J]$	mass matrix of the system
$[K]$	stiffness matrix of the system
X	position vector
$\dot{X}$	velocity vector
$\ddot{X}$	acceleration vector
G_R	shear relaxation modulus
G_∞	long-term shear modulus
G_0	instantaneous shear modulus
G	shear modulus
G'	storage shear modulus
G''	loss shear modulus
g_R	shear relaxation modulus dimensionless
K	bulk modulus
K'	storage bulk modulus
K''	loss bulk modulus
E	tensile modulus
E'	tensile storage modulus
E''	tensile loss modulus
ν	Poisson's ratio
ν'	Poisson's dynamic ratio
ν''	Poisson's loss ratio
σ	stress
ϵ	strain
ϵ_d	strain due to dashpot
ϵ_s	spring due to strain
γ_t	time varying shear strain
τ	reduced time
η	material viscosity
ψ	specific damping capacity
ω_{res}	first natural frequency of the undamped system of resonant vibration
ξ_i	fraction of critical damping
γ_{2xy}	coherence between x and y signals
S_{xx}	auto-spectral density of x signal
S_{xx}	auto-spectral density of y signal
S_{xy}	cross-spectral density between x and y signals
$H(j\omega)$	response function of the system
i	$\sqrt{-1}$
ω	frequency
$\bar{g_i}^P$	Shear modulus Prony series terms
$\bar{k_i}^P$	Bulk modulus Prony series terms
DDL	Damping cork dust layer
DCL	Damping core cork layer

Chapter 1

Introduction

1.1 Introduction

In many systems submitted to dynamic loads the displacements can be higher the wished ones and causing a catastrophic failure that renders useless the structure. In this case it is mandatory to modify the physical structure the system to reduce both the amplitude and time of response to an external excitation.

The methodology for vibration suppression of structures can be classified into three groups, namely passive and active controls or hybrid case which uses both.

1.1.1 Passive control

In passive control the material properties of the structure such as damping and stiffness are modified in order to change the response of structure, consisting basically in increasing the dissipation of energy of the system changing the loss factor for this.
A typical example of passive control is the optimization of the ply-up stacking sequence in composite materials or the study of solid inclusions in the materials.

Composite material parameter

Composites are selected in many structural applications due to their high specific stiffness and strength, hence, the option of passive structural damping is an added advantage to other materials because their properties can

be modified by changing the settings whilst in other materials, such as metals is much more complicated. Recent works of NASA in the damping of unidirectional composites [1] and composite laminates [2] show that composite damping depends on laminate parameters, including constituent material properties, fibber volume ratios, ply orientations, ply thickness, ply stacking sequence, temperature and pre-existing damage.Therefore, in order to obtain significant structural advantages of damping on composite materials,it is very important to use genetic algorithms for optimization purposes, where the variables are the parameters of the laminate. Composite damping is also anisotropic, but exhibits an opposite anisotropy trend than stiffness and strength, being minimum in the direction of the fibers and maximum in the transverse direction and in shear.

Viscoelastic materials

Presently earthquake-resistant design and retrofitting of structures using various energy dissipation devices such as viscoelastic dampers (VEDs), viscous fluid dampers, friction dampers, and added damping and stiffness devices have received considerable attention. Viscoelastics material are able to be used like a damping method because of the higher capacity of dissipating mechanical energy. Since the introduction of this basic concept, many modifications have been proposed to improve the damping performance.

1.1.2 Active control

In active control, structural response is controlled by adding external stresses to the structure using an actuator device, such as a piezoelectric material, located on the surface of component embedded in it. Active control also requires the system to be complex and expensive, despite of one can achieve a good vibration suppression performance compared with passive control.

Depending on the applied voltage, electromechanical coupling of the force transducer to the structure, and the location of the piezoelectric the degree of vibration control of flexible structures can be varied, being a matter for the application of optimization procedures.

1.1.3 Software

For clear reasons one goal of this work was to assess the feasibility of using composite materials with improved damping properties for space applications, in particular in the booms of solar sails which can extend to a signifi-

cant length (15m or more). The experimental analysis necessary to confirm this passive solution is complex, expensive and time consuming. However, the development of a computational model of such a structure constitute a straightforward technique for its dynamic analysis in a few hours. Additionally, many different configurations and variables can be explored leading to a large bulk of data which is crucial for a more efficient design.

Several programs of this type exist on the market like ABAQUS , Ansys or Nastran. In this project we used ABAQUS the commercial FEA sofware of Simulia Company. A virtue of ABAQUS is that it allows a relatively easy modelling of composites and other types of anisotropic materials with great accuracy and versatility of analysis parameters.

1.2 Objectives

The main objective of this project is the study of passive damping systems in structures or mechanical systems that are subjected to loads of any kind which may endanger its strength or cause displacements beyond the design point. The passive method herein here is based on the addition of a layer of viscoelastic material to the primary structure.
In particular, the structure is a CFRP laminate and the layer of viscoelastic material is introduced into the middle-plane in such a way that it allows maintaining symmetry without compromising the strength of the neighbouring regions of the material. Due to its remarkable natural properties, cork was elected as a viscoelastic material to be used in the form of a thin core of a micro-sandwich component.

The energy dissipation effect caused by the viscoelastic layer placed within a flat plate was characterized with a FEM analysis corroborated with the experimental determination of the main dynamic parameters of this configuration of the material. Following this, a computational analysis of a solar sail boom was undertaken in order to get its dynamic response under typical AOCS loads similar to those found in real operational conditions.

1.3 Thesis structure

This project is divided in five chapters including this one.

Capter 2

Chapter 2 is based on a bibliographic review necessary to define the state-of-the-art in the field of passive solutions for vibration control in aeronautical and space structures. He we introduce specific models for damping and viscoelastic behaviour of materials were introduced allowing for a better definition of the assumptions and procedures in the base of the works carried out in this research, namely the proper numerical representation of the materials involved in this project in the context of the considered commercial FEM code.

Chapter 3

Chapter 3 is intended to be a section where they appear in a reasoned manner the imputs to be used in the software. It also contains the geometric description of the specimens used in laboratory tests as well as the boom of a solar sail. It contains all the numerical characterization of mechanical properties of all materials involved, as well as the step-by-step process. Also shown step by Step process of construction and testing of the specimens. In a logical order the mesh characteristics were analysed and a mesh convergence study was undertaken. A final description of the loading and boundary conditions is also made in order to completely define the numerical model.

Chapter 4

The results obtained from the numerical analysis are presented in Chapter 4. Here both the dynamic response to an external load and frequency analysis of the plate and boom configurations are presented, comparing these results to the ones obtained in experimental testing. The results are briefly explained showing the differences amongst the different cases.

Chapter 5

Chapter 5 explains the main ideas extracted from results trying to answer to the initial objectives set for this work. .

Chapter 6

A introduction to future and complementary work is presented.

Chapter 2

Bibliographical review

2.1 General vibration problem formulation

For a general mechanical system with n degrees of freedom the motion equation is given by the equation 2.1.

$$[J]\ddot{X} + [K]X + [F]\dot{X} = [F(t)] \tag{2.1}$$

Where :

- $[J]$,$[F]$,$[K]$,are the mass, damping and stiffness system matrices
- $[F(t)]$ is the external load vector of the finite element model
- $\ddot{X}$,$\dot{X}$,X are the acceleration, velocity and position vectors

Mass and stiffness matrix can be determined from a numerical model implemented using a conventional FEM code(such as ABAQUS).The damping matrix can be treated in two distinct ways. It can be viewed as material property that exists before the implementation of the force vector, thus it is related with the material itself or as purely numerical object that is implemented upon the structure to oppose the excitation force, thus related with the structural characteristics of the vibrating system [3]. Rayleigh damping or proportional damping introduces damping into the vibrating structure, in the form of a damping matrix $[F]$. This concept was introduced first by Rayleigh, who expressed the energy dissipation mechanism responsible of damping, as a symmetric matrix of coefficients. A further idealization to that concept is that the symmetric damping matrix $[F]$ is a linear combination of the mass and the stiffness matrices of the system. Thus, the damping matrix can be defined as

$$[F] = \alpha[J] + \beta[K] \tag{2.2}$$

Where α is the mass proportional damping factor and β is the stiffness proportional damping factor. In the formulation of Rayleigh damping, it is considered that mass proportional damping effect is dominant in the lower frequencies and the stiffness proportional damping is dominant at the higher frequencies. Therefore α and β are the attributes of the lower and higher resonant frequencies, respectively. In this project we consider a boom of a solar sail ,so we can suppose that $\beta \ll 1$ due the typical frequencies in spacial operations.

It can be found [3], that for a given mode i, the fraction of critical damping which is calculated by the commercial finite element code, to obtaining the damped response of the system and considering only the mass proportional damping effect can be defined as

$$\xi_i = \frac{\alpha}{2\omega} \tag{2.3}$$

Further development of the FE methodology for the prediction of damping was based on experimental observations made during vibration damping laboratory testing. Observations were made on the first mode of resonant vibration, which as far as the frequency domain is concerned, it is considered to lie within the range of low frequencies. Therefore, it was considered that the effect of the higher frequency effects was negligible. Hence the mass proportional damping was chosen to represent damping of the vibrating structures. Ultimately only the mass proportional damping factor α would be defined in all finite element models constructed.

It has been well documented [4] that the fraction of critical damping ξ, can be defined in relation to the specific damping capacity ψ of the vibrating structure for a given mode i. Therefore based on experimental calculations of the specific damping capacity (SDC) ψ value, the fraction of critical damping for the first mode of resonant vibration may be defined as

$$\psi = \frac{\xi}{4\pi} \tag{2.4}$$

It is found in literature [4] that equation 2.4, is valid for vibrating systems that demonstrate a value of $\psi < 100$.

Thus by calculating the fraction of critical damping for the first mode of resonant vibration from equation 2.4,the mass proportional damping factor α may be expressed as

$$\alpha = 2\xi\omega_{res} \tag{2.5}$$

In the above equation ω_{res} is the natural frequency of the undamped system for the first mode of resonant vibration. It is calculated as the square root of the eigenvalue in the eigenvalue extraction step prior to the steady

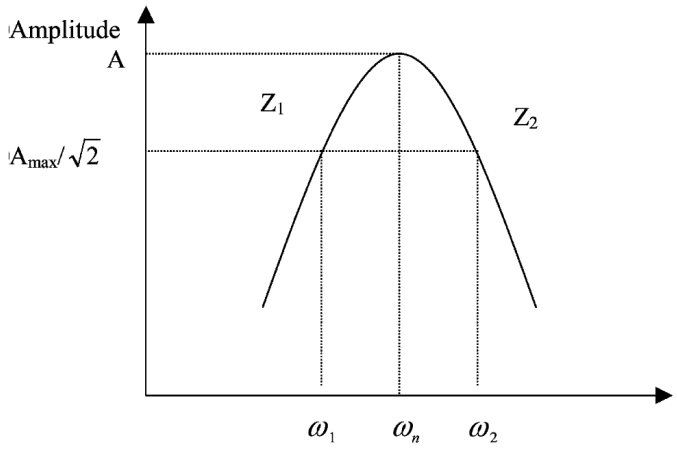

Figure 2.1: Half-power bandwidth method

state dynamics step. It is quite clear that for a given finite element model with certain mass and stiffness matrices, the results of the dynamic analysis depend hugely on the numerical assignment of the α and β parameters. It is of significant importance that the numerical values assigned to α should be based on experimental data.

2.1.1 Modal data extraction

In the present case, the bandwidth method was used to determine damping. Measuring frequency bandwidth, between points on the response curve, for which the response is some fraction of the resonance of the system. The usual convention is to consider points Z1 and Z2 as in indicated in 2.1, to be located at frequencies on the response curve where the amplitude of response of these points is $\frac{1}{\sqrt{2}}$ the maximum amplitude. The bandwidth at these points is known as half-power bandwidth. The half-power points or 3 dB points for small damping correspond to the frequencies $\omega_1 = \omega_n(1-\xi)$ and $\omega_2 = \omega_n(1+\xi)$ where ξ is the damping ratio mentioned above. The frequency interval between this two points is $\Delta\omega = \omega_2 - \omega_1$ The loss factor is defined by equation 2.6

$$2\xi = \frac{\Delta\omega}{\omega_n} \tag{2.6}$$

2.1.2 Random signal analysis in testing

The transducer used to measure booth the input and output during a vibration test usually contains noise from different sources and complicate the analysis of the data. Thus it is important to consider the random input vibration response [5].

The autocorrelation of a signal and the associated power spectral density (PSD) are given by equations 2.7 and 2.8

$$R_{xx}(\tau) = \lim_{T\to\infty} \frac{1}{T} \int_0^T x(t)(\tau)x(t+\tau)\, dt \tag{2.7}$$

$$S_{xx}(\omega) = \frac{1}{2\pi} \int_{-\infty}^{\infty} R_{xx}(\tau)e^{-j\omega t}\, d\tau \tag{2.8}$$

It is know that the PSD of the input driving force can be related to the PSD of the response and the frequency response function of the system by equation2.9

$$S_{xx}(\omega) =\mid H(\omega) \mid^2 S_{yy}(\omega) \tag{2.9}$$

were $H(\omega) = \dfrac{1}{k - m\omega^2 + c\omega j}$ is the response function of the system.

The frequency response function can also be related to the cross correlations between the two signal x(t) and y(t). The cross correlation function, denoted $R_{xy}(\tau)$ for the two signals x(t) and y(t) is defined by equation 2.10

$$R_{xy}(\tau) = \lim_{T\to\infty} \frac{1}{T} \int_0^T x(t)(\tau)y(t+\tau)\, dt \tag{2.10}$$

$$S_{xy}(\omega) = \frac{1}{2\pi} \int_{-\infty}^{\infty} R_{xy}(\tau)e^{-j\omega t}\, d\tau \tag{2.11}$$

These correlation and density functions also allow calculating the transfer functions of the structures submitted to the tests. The frequency response function is related to the spectral density functions by the equations 2.12 and 2.13

$$S_{yx}(\omega) = H(j\omega)S_{yy}(\omega) \tag{2.12}$$

$$S_{xx}(\omega) = H(j\omega)S_{xy}(\omega) \tag{2.13}$$

The coherence function denoted by γ^2 is defined to be the ratio of the two values of $H(j\omega)$ is defined by equation 2.14

$$\gamma^2 = \frac{|S_{xy}(\omega)|^2}{S_{xx}(\omega)S_{yy}(\omega)} \tag{2.14}$$

which always lies between 0 and 1. In fact, if the measurements are consistent, $H(j\omega)$ should be the same value, independent of how it is calculated and the noise of the signal. If it is 0 the measurement is of a pure noise; if the value of coherence is 1, the signals x and y are affected by noise. In practice coherence versus frequency is taken as an indication of how accurate the measurement process is over a given range of frequencies. Generally the values closer to one should occur at values of ω near the structure's resonant frequencies. Near resonance the signals are large and hence less affected by noise. In practice, data with a coherence of less than 0.75 are not used and indicate that the test should be done over.

2.1.3 Eigenvalues problem formulation

Eigenvalues of undamped system are given by

$$[J]\ddot{X} + [K]\dot{X} = [0] \tag{2.15}$$

In the other hand if we suppose a harmonic response

$$X = [\phi] \exp^{i\omega t} \tag{2.16}$$

Finally using equation 2.16 in 2.15

$$|[k] - \lambda[J]| = [0] \tag{2.17}$$

were λ is ω^2 and λ_i the eigenvalues of the system. For a general system with damping the natural frequencies are given by

$$\omega_d = \omega_{nd}\sqrt{1 - \xi^2} \tag{2.18}$$

2.2 Viscoelastic materials

The general development and application of the linear theory of viscoelasticity had its origin in the development and widespread use of polymeric materials. The theory of viscoelasticity may account for materials which posses a capacity to both store and dissipate mechanical energy.These materials for a which a suddenly applied and maintained state of uniform shear stress by a steady flow process which may or may not be limited in magnitude as time grows and is said to exhibit both an instantaneous elasticity effect and creep characteristics. This behaviour is clearly not described by either an elasticity or viscosity theory but combines features of each. Christiensen (1971)[6] argues that this type of material possesses a characteristic which

can be descriptively referred to as a memory effect. That is the material response is not only determined but the current state of stress, but is also determined by all past states of stress, and in general sense, the material has a memory for all past states of stress.

All real solid materials possess both elastic and damping properties. Damping is the ability to dissipate some mechanical energy during vibration or dynamic deformation.

When analyzing materials with time dependent mechanical properties, it is of vital importance that the characterization of such properties be accurately defined. For viscoelastic materials, properties such as relaxation modulus, creep compliance, and time-dependent Poisson's ratio are of utmost importance for numerical and closed form solutions to various problems,[7].

A homogeneous, isotropic solid material is known to have two independent complex moduli, namely the complex shear modulus, $\bar{G}$, and the bulk modulus, $\bar{K}$ suffice for a complete description of the viscoelastic behaviour (equations 2.19 and 2.20). The only requirements regarding the form of a complex modulus is that both its real and imaginary part is non negative.This is a consequence of the requirements of non negative energy storage and non negative energy dissipation. The complex Poisson's ratio and the complex tensile modulus for homogeneous, isotropic, linear solid viscoelastic materials is given by equations 2.22 and 2.21.

$$\bar{G}(j\omega) = G'(\omega) + jG''(\omega) \tag{2.19}$$

$$\bar{K}(j\omega) = K'(\omega) + jK''(\omega) \tag{2.20}$$

$$\bar{E}(j\omega) = E'(\omega) + jE''(\omega) \tag{2.21}$$

$$\bar{\nu}(j\omega) = \nu'(\omega) + j\nu''(\omega) \tag{2.22}$$

Where E',G',K' are the storage components and E",G",K" are the loss components.

In the complex Poisson's ratio ν' and ν'' are the dynamic and the loss component respectively. Pritz (2007) [8] analyses the importance of complex Poisson's ratio in the the linear dynamic behaviour of solid materials.He concludes that magnitude of the Poisson's loss factor normally does not exceed 0.1 even if the shear damping is high; furthermore the Poisson's loss factor of a high loss rubbery material may be much smaller than 0.1 if ν' is close

to 0.5 or zero.

If we have $\bar{E}$ and $\bar{\nu}$ we can obtain the $\bar{G}$ and $\bar{K}$ values quite closely with the following relations like in [9]:

$$\bar{G} = \frac{\bar{E}}{2(1+\bar{\nu})} \tag{2.23}$$

$$\bar{K} = \frac{\bar{E}}{3(1-2\bar{\nu})} \tag{2.24}$$

2.2.1 Mathematical models for linear viscoelastic response

The way to model a viscoelastic material is very similar to electric circuit but in this case we have two components corresponding to the elastic term and another to the viscous term. The elastic components, as previously mentioned, can be modeled as springs of elastic constant E, given by

$$\sigma = E\epsilon \tag{2.25}$$

where σ is the stress, E is the elastic modulus of the material, and ϵ is the strain that occurs under the given stress. The viscous components can be modelled as dashpots such that the stress-strain rate relationship can be given as

$$\sigma = \eta\dot{\epsilon} \tag{2.26}$$

where σ is the stress, η is the viscosity of the material, and $\dot{\epsilon}$ is the time derivative of strain. The spring models the instantaneous bond deformation of the material, and its magnitude will be related to the fraction of mechanical energy stored reversibly as strain energy and the entropic uncoiling process is fluid like in nature, and can be modelled by a Newtonian dashpot. There are a large number of models used to simulate the wide range of viscoelastic materials that are being each used for a given material and conditions.

- The Maxwell model
  is a mechanical model in which a "Hookean" spring and a Newtonian dashpot are connected in series so the stress on each element is the same and equal to the imposed stress, while the total strain is the sum of the strain in each element.

$$\sigma = \sigma_s = \sigma_d \tag{2.27}$$

$$\epsilon = \epsilon_s + \epsilon_d \tag{2.28}$$

Here the subscripts $_s$ and $_d$ represent the spring and dashpot, respectively. It is convenient to differentiate the strain equation and then write the spring and dashpot strain rates in terms of the stress, thus obtain the differential equation model give by 2.29

$$\dot{\epsilon} = \dot{\epsilon_s} + \dot{\epsilon_d} = \frac{\sigma}{\eta} + \frac{1}{E}\dot{\sigma} \tag{2.29}$$

Under this model, if the material is put under a constant strain, the stresses gradually relax, when a material is put under a constant stress, the strain has two components. First, an elastic component occurs instantaneously, corresponding to the spring, and relaxes immediately upon release of the stress. The second is a viscous component that grows with time as long as the stress is applied. The Maxwell model predicts that stress decays exponentially with time, which is accurate for most polymers. One limitation of this model is that it does not predict creep accurately. The Maxwell model for creep or constant-stress conditions postulates that strain will increase linearly with time. However, polymers for the most part show the strain rate to be decreasing with time. Application to soft solids such thermoplastic polymers in the vicinity of their melting temperature,numerous metals at a temperature close to their melting point.

- The Kelvin-Voigt model
  It consists of a Newtonian damper and "Hookean" elastic spring connected in parallel. The constitutive relation is expressed as a linear first-order differential equation

$$\sigma = E\epsilon + \eta\dot{\epsilon} \tag{2.30}$$

  This model represents a solid undergoing reversible, viscoelastic strain. Upon application of a constant stress, the material deforms at a decreasing rate, asymptotically approaching the steady-state strain. When the stress is released, the material gradually relaxes to its undeformed state.The model is extremely good with modelling creep in materials, but with regards to relaxation the model is much less accurate. This model is useful to simulate organic polymers, rubber, wood when the load is not too high.

- The standard linear solid
  Most polymers do not exhibit the unrestricted flow permitted by the

Maxwell model, although it might be a reasonable model for warm tar. For more typical polymers whose conformational change is eventually limited by the network of entanglements or other types of junction points, more elaborate spring-dashpot models can be used effectively. This model consists of adding a spring in parallel with the Maxwell model that provides an equilibrium or rubbery stiffness that remains after the stresses in the Maxwell arm have relaxed away as the dashpot extends. The diferential equation for this model is:

$$\dot{\epsilon} = \frac{\frac{E_2}{\eta}(\frac{\eta}{E_2})\dot{\sigma} - E_1\epsilon}{E_1 + E_2} \tag{2.31}$$

- The Maxwell-Wiechert model
  A real polymer does not relax with a single relaxation time as predicted by the previous models. Molecular segments of varying length contribute to the relaxation, with the simpler and shorter segments relaxing much more quickly than the long ones. This leads to a distribution of relaxation times, which in turn produces a relaxation spread over a much longer time than can be modeled accurately with a single relaxation time.The model have many spring-dashpot Maxwell elements as are needed to approximate the distribution satisfactorily.

2.2.2 The Boltzman superposition integral

Using formulation the Boltzmann's superposition principle such that the current stress is determined by the superposition of the responses to the complete spectrum of increment strains,the basic hereditary integral formulation for linear isotropic viscoelasticity is :

$$\sigma(t) = \int_0^t 2G(\tau - \tau')\dot{e}\, dt' + I\int_0^t 2G(\tau - \tau')\dot{\phi}\, dt' \tag{2.32}$$

where $\dot{e}$ and $\dot{\phi}$ are the mechanical deviatoric and volumetric strains; K is the bulk modulus and G is the shear modulus, which are functions of the reduced time τ; and . denotes differentiation with respect to t'. The reduced time is related to the actual time through the integral differential equation.Note that the notation used is is similar to the one used in ABAQUS [10].

In this case we suppose small strain. Consider a shear test at small strain, in which a time varying shear strain, ϵ_t, is applied to the material.

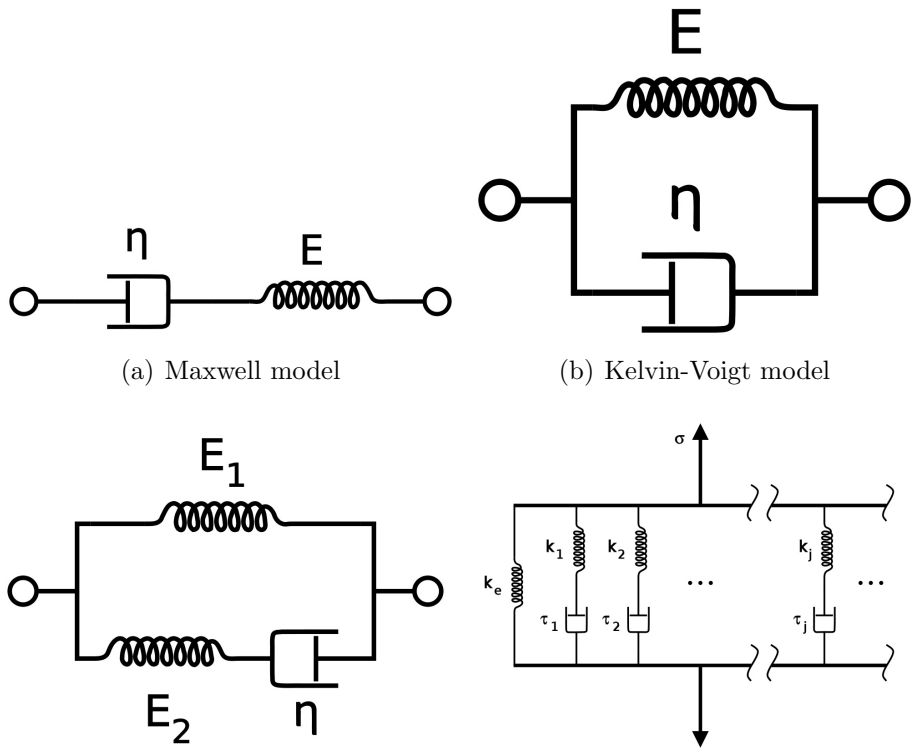

(a) Maxwell model (b) Kelvin-Voigt model

(c) Standard linear solid model (d) Maxwell-Wiechert model

Figure 2.2: Different viscoelastic models

The response is the shear stress $\tau(t)$. The viscoelastic material model defines $\tau(t)$ as

$$\tau(t) = \int_0^t G_R(\tau - s)\dot{\epsilon(s)}\, ds \tag{2.33}$$

where G_R is the time-dependent shear relaxation modulus that characterizes the material's response.This constitutive behaviour can be illustrated by considering a relaxation test in which a strain ϵ is suddenly applied to a specimen and then held constant for a long time. The beginning of the experiment, when the strain is suddenly applied, is taken as zero time, so that

$$\tau(t) = \int_0^t G_R(\tau - s)\dot{\epsilon}(s)\, ds = G_R\epsilon(since\dot{\epsilon} = 0; t > 0) \tag{2.34}$$

where ϵ is the fixed strain. The viscoelastic material model is long-term elastic in the sense that, after having been subjected to a constant strain for

a very long time, the response settles down to a constant stress; $G_R(t) \to G_\infty$ as $t \mapsto \infty$

The shear relaxation modulus can be written in dimensionless form:

$$g_R(t) = \frac{G_R(t)}{G_0} \tag{2.35}$$

where $G_0 = G_R(0)$ is the instantaneous shear modulus, so that the expression for the stress takes the form

$$\tau(t) = G_0 \int_0^t g_R(\tau - s)\dot{\epsilon(s)}\, ds \tag{2.36}$$

The dimensionless relaxation function has the limiting $g_R(0) = 1$ values and $g_R(\infty) = \dfrac{G_\infty}{G_0}$

A popular method of obtaining analytical expressions for these properties consists of obtaining discrete values as a function of the logarithm of time and curve fitting the data to an appropriate expression. Due to the decaying nature of such properties as Relaxation Modulus and Poisson's Ratio, they are conveniently represented as a series of exponential functions. A widely used form of these functions is the so-called Prony series (due to Gaspard Francois Clair Marie Riche de Prony, 1755- 1839), which can be expressed as

$$\bar{f} = A + \sum_{i=1}^{n} B_i e^{\epsilon_i t} \tag{2.37}$$

When using expressions such as this for curve fitting it is noted that there are too many unknowns for the amount of equations available for simultaneous solving. This generally leads to a trial and error approach where values of ϵ_i are assumed, and an expression for the time-dependent variable is obtained repeated until a satisfactory curve fit has been obtained.

ABAQUS [10], assumes that the viscoelastic material is defined by a Prony series expansion of the dimensionless relaxation modulus:

$$g_R(t) = 1 - \sum_{i=1}^{N} \bar{g_i}^P (1 - e^{\frac{-t}{\tau_i^G}}) \tag{2.38}$$

$$k_R(t) = 1 - \sum_{i=1}^{N} \bar{k_i}^P (1 - e^{\frac{-t}{\tau_i^G}}) \tag{2.39}$$

Where N, $\bar{g_i}^P$,$\bar{k_i}^P$,τ_i^G,i= 1,2,...,N are material constants.

Using Fourier transforms, the expression for the time-dependent shear modulus can be written in the frequency domain as follows.

$$G_s(\omega) = G_0[1 - \sum_{i=1}^{N} \bar{g_i}^P] + G_0 \sum_{i=1}^{N} \frac{\bar{g_i}^P \tau_i^2 \omega^2}{1 + \tau_i^2 \omega^2} \tag{2.40}$$

$$G_l(\omega) = G_0 \sum_{i=1}^{N} \frac{\bar{g_i}^P \tau_i \omega}{1 + \tau_i^2 \omega^2} \tag{2.41}$$

$$K_s(\omega) = K_0[1 - \sum_{i=1}^{N} \bar{k_i}^P] + K_0 \sum_{i=1}^{N} \frac{\bar{k_i}^P \tau_i^2 \omega^2}{1 + \tau_i^2 \omega^2} \tag{2.42}$$

$$K_l(\omega) = K_0 \sum_{i=1}^{N} \frac{\bar{k_i}^P \tau_i \omega}{1 + \tau_i^2 \omega^2} \tag{2.43}$$

Where G_s,G_l,K_s and K_l are the shear storage modulus,the shear loss modulus, the bulk storage modulus and the bulk loss modulus.

2.3 Historic problems

Dynamic control of structures is one of the main problems of this industrialized and technical society.Resonance's problems are normally present in mechanic systems, structures and also in the nature.

- In machinery design there is always risk of resonance between rotation frequency of the rotatory parts and one of the vibration modes of the whole structure. This is inevitable because when accelerating or braking there is a large probability of going through a natural frequency of the structure.If this comes to be one of the main modes, one can try to changing this frequency by varying the stiffness or introducing damping. This extends to the buildings in which machinery is installed: normally the engine must be mounted on isolators. The engine of a car is mounted on rubber pads so it will not transmit vibrations to the chassis.

- Wind can also produce resonances. In 1879 the bridge over Tay river,in Scotland, sank to the passage of a train killing 75 people.In 1940 Tacomas suspension bridge collapsed in the USA. The failure was caused by resonance between the vibrations of the suspension cables in the wake of karman vortex arising with strong wind.These oscillations produce a torsion in the bridge deck,till its catastrophic failure. Others say it

was the board itself that entered a similar resonance to flutter. In 2000 the London's Millennium Bridge which is a pedestrian bridge designed by the renowned architect Norman Foster. Two days after it had to close because, when passing a large number of people, ranging laterally resonance with the steps. It took two years to design and install a solution using viscous dampers to overcome this situation.

- Technology deficiencies were identified in several studies on large space systems (LSS) conducted by NASA in the 60's and 70's [11]. The results were concibed for space applications by the year 2000.

2.4 Evolution of the different technical solutions

The techniques most used and most successful in this field have their beginning in the 50s. Oberst (1952) proposed to apply a thin layer of viscoelastic material to the surface of flexible structures for vibration control.

Ungar and Ross (1959) [12] suggested a multiple constrained layer treatment and their analyses shows that the increase of the number of viscoelastic layers may be negligible at high frequencies; however this effect can be quite considerable at low frequencies especially for a large number of layers (fig.2.6).The damping characteristics of a damping layer treatment is determined by the sum of all constraining layers; the number of tapes used and their relative thicknesses have only a small effect. The previous conclusion can be very useful from the practical point of view in the construction of a structure.

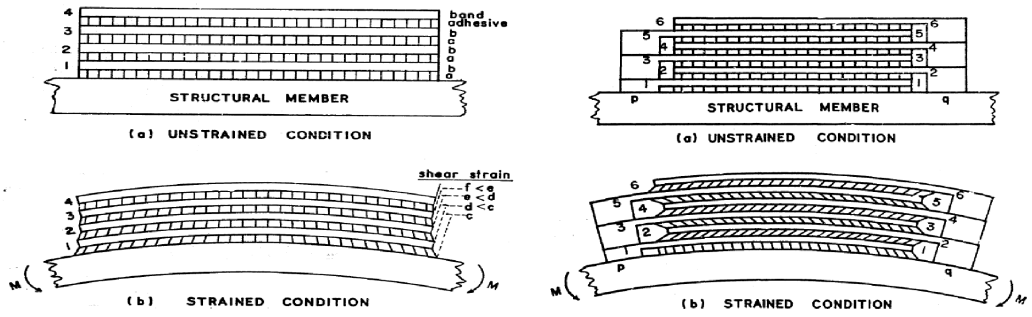

Figure 2.3: Different damping layers configuration

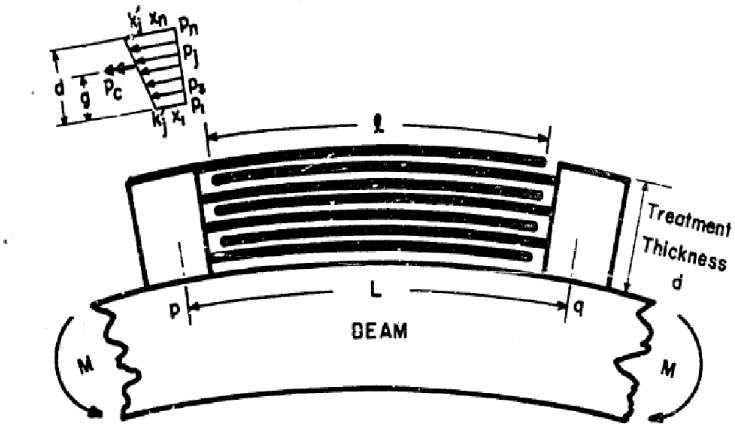

Figure 2.4: Thick treatment geometry and displacement distribution under flexure

Lazan, Metherell and Sokothe (1965) [13] presented a demonstration that configuration of multiple-band surface treatment is capable of dissipating significantly more energy than conventional free or constrained layer treatments.

Schubert et al. (1967)[14] make a theoretical study to evaluate the geometrical parameter of structural composites with viscoelastic shear damping mechanisms.Also of design equations and graphs for the geometrical parameter for a large number of designs with different configurations of the viscoelastic layer and which are potentially used. These authors came to a automated process allowing the determination of the loss factor for a with a constrained viscoelastic layer between elastic elements.

Plunkett and Lee (1969) [15] investigate about the constrained viscoelastic damping, in which the viscoelastic layer is covered in turn by a high tensile stiffness constraining layer. The constraining layer induces shear strain in the viscoelastic layer, and thus greater damping is produced.A important result give by the analysis is that,for optimum element length of the constraining layer,the energy dissipation depends primarily of the loss coefficient of the viscoelastic material, and the stiffness of the contraining layer and only indirectly on the shear modulus of the viscoelastic layer (fig 2.5).

For the enhanced damping material we can mention the model described in U.S. Patent 5.203.435 (1993) [16] using a layer of viscoelastic combined with a zig-zag configuration of the fiber alignment. The fiber enhanced vis-

coelastic damping treatment represents both substantial increase in damping and decrease in weight added when compared with conventionally constrained viscoelastic layered damping treatment (fig 2.7).

In the research dealing with the combination of composite materials with different damping properties it is worthwhile to mention the work of Woo Young and Amjad [11]. Within the field of optimization we can cite Mota Soares et al.(2008)[17] where constrained optimization of passive damping is conducted for the maximization of modal loss factors, using the Feasible Arc Interior Point Algorithm (FAIPA) to get the best configuration of the layers.

In a specific study of a solar sail boom to better understand the current state of the art and standardized tests and static and dynamic.In [18] authors examine examines the use of booms consisting of two co-bonded omega shaped carbon fiber half shells with 0.1 mm wall thickness each and had a weight of only 62 g per meter.

Sickinger et all(2009) [19]. pointed out that that it is expected that mass reductions can be achieved in the deployable booms by means of a tapered design over the boom length. They have shown that the load is not homogeneously distributed over the boom lengths. The bending moments that are particularly important for the design become increasingly smaller the closer they get to the boom tips.

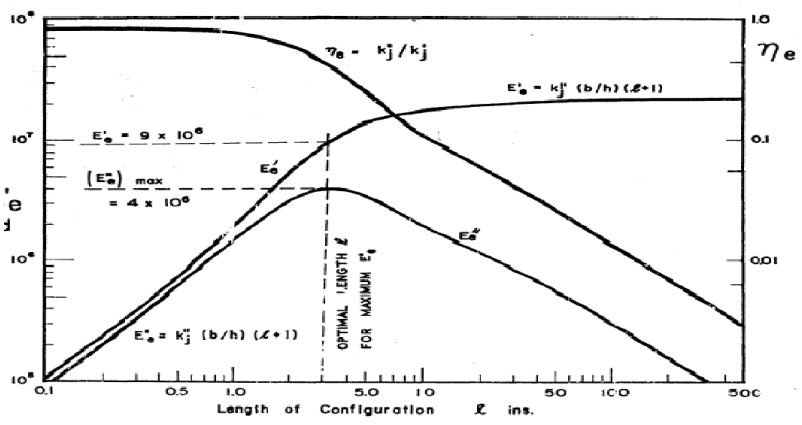

Figure 2.5: Loss factor,equivalent storage and loss modulus

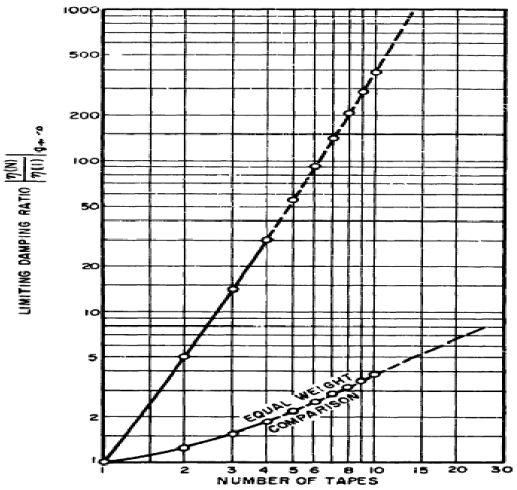

Figure 2.6: Low frequency advantage for multiple layers

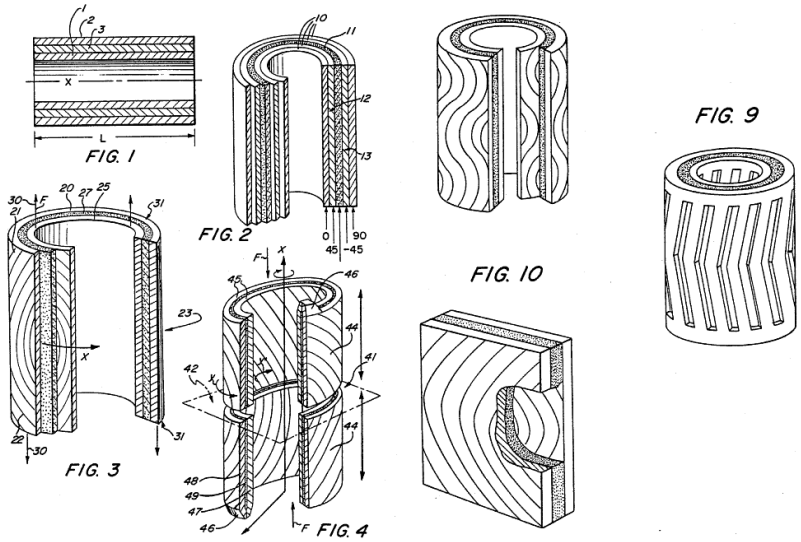

Figure 2.7: Composite damping struts for large precision structures

2.5 Material selection

With regards to the material used for damping the final choice has been relaying upon cork.Cork is natural material obtained from cork tree mostly in Mediterranean countries, mainly in Portugal and Spain which are the world's main producers [20]. The special combination of properties of cork has have been exploited since ancient times by man.Since the construction of small boats and fishing until kits use in domestic kitchen sets and containers for food and liquids, several applications can be found on a regular basis.. But undoubtedly the most important application to date is the use of cork to produce wine bottle stoppers.

At present, apart from this latter application the use of cork based products is mainly confined to the acoustic and thermal insulation of buildings and, in a much lesser extent, shoes and garment ornaments.

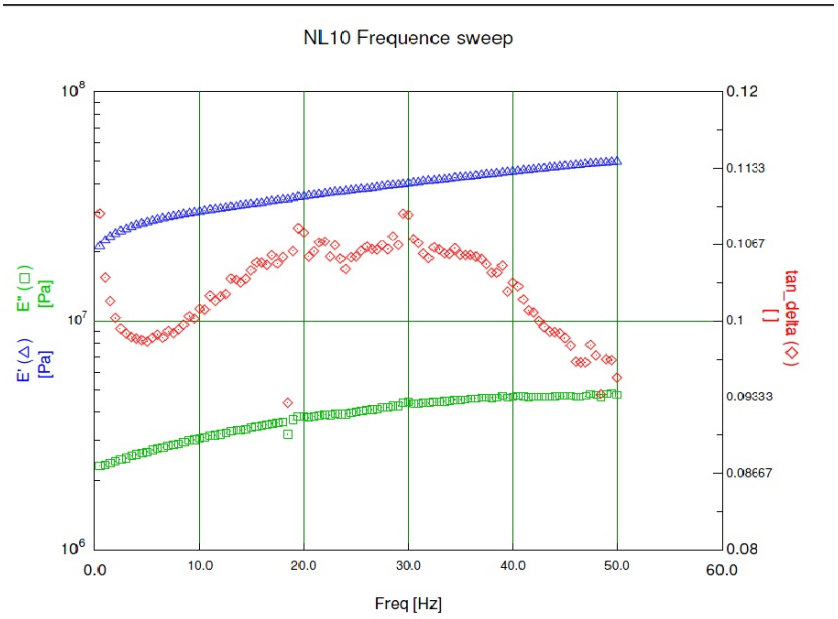

Figure 2.8: DMA spectra in frequency sweep

Mano (2002) [21] showed that viscoelastic properties of cork are anisotropic and the higher values of the storage modulus are found when the material is oriented along the transverse prismatic direction.In his numerical work a cork based sandwich has been used, which unlike natural cork has a more uniform that allow considering isotropic conditions in the performed simulations (fig 2.8).

The sandwich components with cork agglomerates layers have an high

energy absorption capacity with minimum damage probability, resulting in better crash worthiness properties when impact loading is expected during service as shown in Castro et al.(2010)[22].This property is useful in space applications, where the life of the structure is essential and many of the loads on structures can be considered as impulsive loads, due to it occur in very small periods of time. Gameiro et al.(2007)[23] suggest that micro-agglomerate cork may become the adequate material for innovative applications that require low cost, low density and high energy absorption and may be a very interesting material to use in applications where strain rate sensitivity is undesirable.

Chapter 3

Numerical model

3.1 Introduction

The main problem studied in this project is use passive methods to reduce the magnitude of displacement ad also the harmful and unwanted vibrations for any structure that requires it. We will use the FEA software to model and simulate numerically a plate. Likewise, the intention to make an approach for space applications, particularly in solar sail boom dynamic control. The most important part of this chapter is to obtain all the inputs in a reasoned way, needed to do the simulation in both cases. This requires a thorough knowledge of both models, the boundary conditions and the loads which are it are subjected. Obviously if the boom is much more complex from the standpoint of a correct simulation.

3.2 Materials and configuration

The base material use for both plate and boom is TEXIPREG®HS 160 REM epoxy CFRP and the materials used for the damping layer are a core cork type NL10 and a granulated cork both provided by Amorim Cork Composites Company. The mechanical properties of each one are shown in table [**?**].

Regarding to the loss factor of each material to be used in the numerical

Material	$\rho(\frac{Kg}{m^3})$	ν	E(Mpa)	G(Mpa)	α
CFRP	1000	0.25	150000	5000	6.4
Cork	140	0.1	0.6	5.9	20

Table 3.1: Material properties

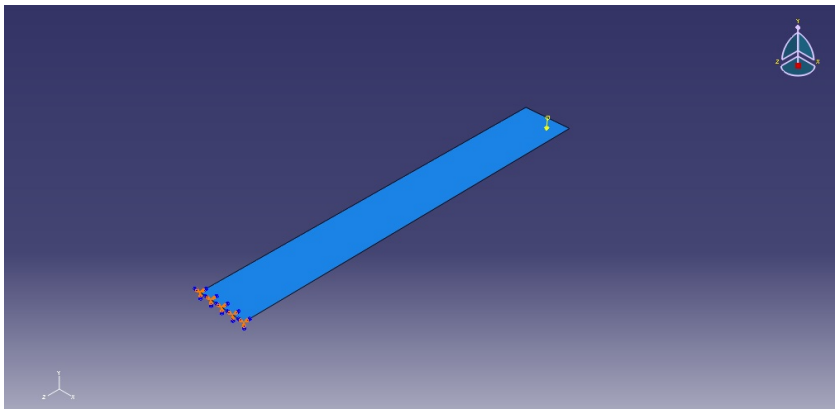

Figure 3.1: Plate model in ABAQUS

simulation is taken into account that the objective of the project is focused on low frequencies,this parameter is determined using the figure provided by Amorim cork composites fig. 2.8 and the equation 2.5.

3.3 Plate model features

The plate used is a simple plane model embedded in one end and subjected to an impulsive point load considered. It is made of CFRP laminate, and then will be added a layer of core cork in the symmetry zone to compare results and see the effects that this causes. The dimensions are 450 mm x 60 mm and distribution of the layers is the following :

$[0_2\ 90_2\ 0\ 90]_s$

Should be noted that the width of each layer when cured CFRP is 0.15 mm.

3.3.1 Loads and boundary conditions

The plate is considered fixed at one of its ends and subjected to an impulsive point load of 1 N applied at the center of the opposite end. This load is simulated using a range of application of the same very small in this case 0.05 s. Has been careful not to impose a very high load value to avoid large displacements to ensure compliance of the linear theory.

Experimental test

To know as best as possible the real properties of the materials used in project we make a laboratory tests. Three different configurations of plates will test:

- CFRP
- CFRP with a cork core layer
- CFRP with granulated cork layer agglomerate

Four specimens of each type to be submitted to different tests in order to have greater confidence in results.

The prepreg TEXIPREG®HS 160 REM is a hight strength unidirectional carbon prepreg with modified epoxy resin REC, suitable both for compression and vacuum-bag moulding. It issues directly to the honeycomb and it does not need any adhesive film for sandwich moulding. Well fitted for top-class fishing rods sport tools. First the prepreg is extracted from the freezer and let it temper at least two hours in its protective packaging. The necessary material is cut and the rest is stored again.The orientations used in the specimens are 0 and 90 for simplicity and due to time.The dimensions of all the specimens are 450 mm x 60 mm.

CFRP

The stacking sequence is $[\ 0_2\ 90\ 0\ 90]_s$ and only is necessary paste the different layers.

CFRP with cork core layer

The stacking sequence is $[0\ 90\ 0\ \mathrm{DCL}\ ]_s$. The fabrication procedure is followed as in the previous case with the difference that now a core cork layer will be added with caution to achieve good union among the two materials and the addition of resin for this purpose.

CFRP with granulated cork layer agglomerate

In this case has to be done uniform layer of granulated cork. Note that the cork has been mixed with epoxy resin in advance. The configuration used is $[0_2\ 90\ \mathrm{DDL}\ 90\ 0_2\ 90\ ]_s$

Autoclave cycle

- make the bag and apply 0.5 bar vacuum
- heat to 125 at 3-5 / min rate
- when 120-125 is reached apply 2-7 bar

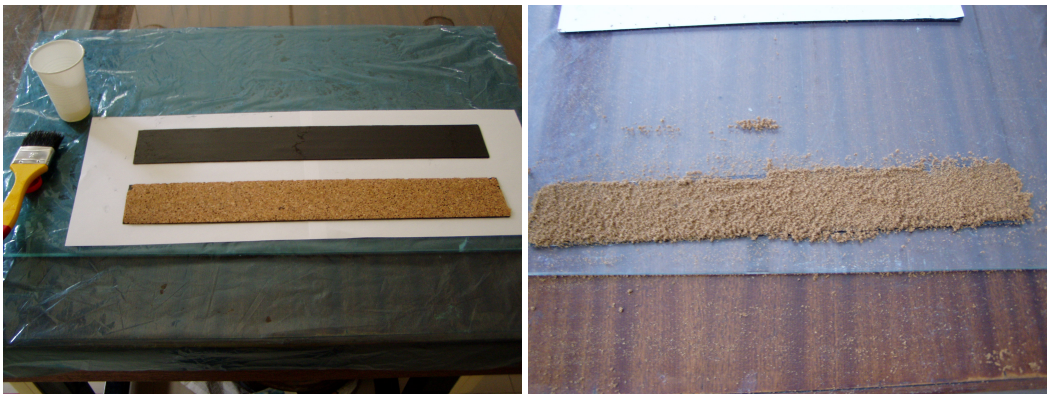

Figure 3.2: manufacture of the different specimens; with cork sandwich and with cork dust

- maintain pressure and temperature for 60'
- get the part out from the mould

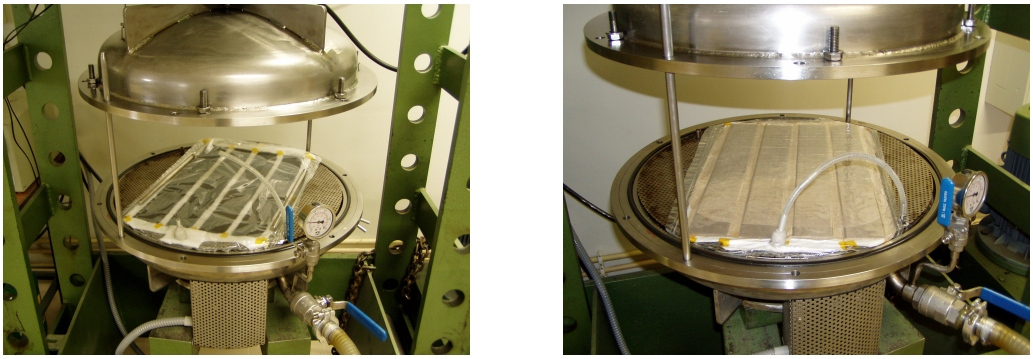

Figure 3.3: Specimens in the autoclave to begin the curing process

Finally with the help of sandpaper and a cutter to prepare the specimens to be tested and conducted a series of measures both the thickness and width. After carefully labeled the specimens were subjected to test in the Instituto Politécnico de Setúbal (IPS) labs. The test consisted basically in determining the loss factor of different configurations by bandwidth method, and and thus obtain the mass proportional damping factor α for use in the FEA model, all this following the standard AST E796-98. The specimens are placed suspended on two nylon threads and struck with a hammer to excite different modes in a range of frequencies from 0 to 1500 Hz.With an

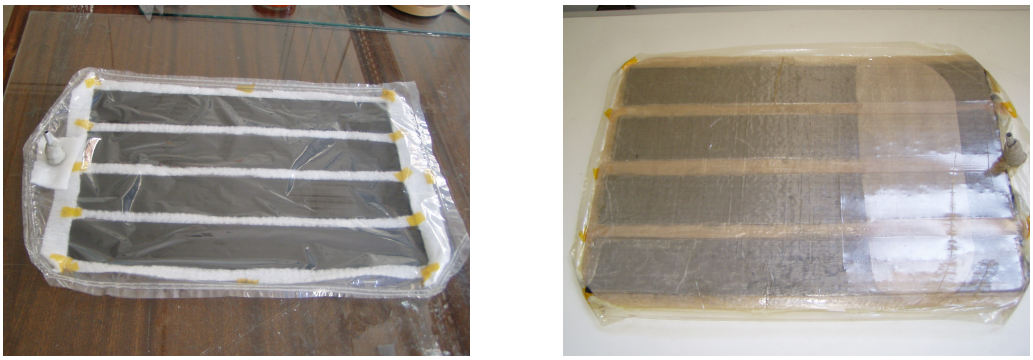

Figure 3.4: Specimens before and after the curing process

accelerometer located at the opposite end to which the response we get hit in frequency by two successive integrations.With an accelerometer located on the opposite side which we hit we obtain the frequency response by two successive integrations. Also we obtain the hammer impact characteristics by a sensor on the face where we hit.In the display both responses are represented as well as coherence equation 2.14.Four tests are made with each specimen. We performed a series of ten shots in each that are recorded on the transducer taking care to validate the shock when the coherence is close to unity and the rest manually voiding that produce much lower values.to eliminate undesirable noise that get worse the results take special care in the fixation of the specimens in the nylon thread and the placement of the accelerometer. This was placed at the opposite side to avoid saturation of the accelerometer produced at impact. The data are processed on a computer using the software Vibpro (fig.3.6) and LabView (fig.3.7). The first for for preprocessing of the data and obtain the representation of frequency response. And the LabView is used to determine the loss factor at frequencies of using a routine created by the Dr. Ricardo Cláudio professor of ITS in Setúbal, using an algorithm to obtain automatically points 3dB below the maximum, having the possibility of a manual adjustment for greater precision.We realize the calculations 3db and 6db and we make sure that the values the loss factor for each of the frequencies did not change greatly from one to another case, signal that have high stability and are formally valid. He also took care to eliminate loss factor values associated with the first resonance frequency. The results in each case are shown in the following tables.

Table 3.2: Loss factor for simple CFRP specimens C1

frequencies	loss factor
81.59821	0.0188975
224.62692	0.006995
440.2905	0.0035475
727.3905	0.0034525
1080.55554	0.0028425
1499.52698	0.00235

Table 3.3: Loss factor for simple CFRP specimens C2

frequencies	loss factor
81.43372	0.0199675
223.71077	0.00681
720.5578	0.003
1073.5144	0.0027125
1489.51001	0.00235

3.4 Boom model features

Structural and Mechanical design

One of the most fundamental structural and mechanical trades is the implementation of the deployable boom for the square sail, as on a sailing ship, the unfolding of sails requires suitable rigid structures, i.e. booms. These these could be one of the next

- Pantographic structures, which consist of rigid links with hinges in between
- Inflatable structures stabilized by internal gas pressure
- Morphing structures which exist in two stable geometrical states,one for the stowed and one for the deployed configuration,and can be converted from one to the other

.Carbon lenticular foldable elastic tubes were chosen over inflatable booms because the are more mature technology with well understood properties. We based our reference design on booms developed by DLR for a 14 length

Table 3.4: Loss factor for simple CFRP specimens C3

frequencies	loss factor
82.54212	0.0206
226.71335	0.0071375
442.69293	0.0037
728.38629	0.0032
1084.51013	0.0028675
1502.52991	0.002475

Table 3.5: Loss factor for specimen with cork core S1

frequencies	loss factor
100.32729	0.024005
280.54694	0.0111125
534.55493	0.0087875
852.51587	0.01036
1226.5094	0.01315

booms. This design provides for storage of the rolled up booms on a single large central reel and a motor driven deployment that is well controlled but this last detail does not matter because the analysis is done with the mast is fully deployed.

Boom geometry

In the analysis we consider a boom length of 14 m and the classical section in OMEGA. The model is same that exist in the AEROUBI laboratory. DLR is currently working in ultra-light poles with a single layer thickness of 0.1 mm but here we use a base thickness of 0.3 mm and used a number of layers, thickness and orientation of them as parameters of the problem for optimize the damping of the boom. In the numerical example we use the configuration $[45\ -45]$ for the simple boom and $[45\ DCL\ -45]$ for the boom with the passive damping system. Although this kind of product not known, the layer of cork is considered as sandwich of 0.1 mm to correspond to a model of boom reasonable and useful, since the use of current commercial thickness, resulting in a total thickness that will almost certainly prevent the proper storage and deployment of the boom, also a thick cork excessively

Table 3.6: Loss factor for specimen with cork core S2

frequencies	loss factor
101.56985	0.01945
276.70654	0.0080725
531.4223	0.0076225
861.4826	0.011485
1255.50854	0.010265

Table 3.7: Loss factor for specimen with cork core S3

frequencies	loss factor
102.68484	0.0230875
290.66422	0.0088175
557.5772	0.0076675
892.50641	0.0117375
1270.48999	0.011675

reduce the stiffness and strength of the structure making it unviable.

3.4.1 Loads and boundary conditions

To know the loads applied on the boom, it is necessary to understand the functioning of the AOCS because it is the main source. A number of options for attitude control of the deployed sail is considered. Purely propellantless either options were based on shifting the center of mass relative to the center of pressure relative to the center of mass. For the latter, we consider using articulates vanes and also articulated the sail panels themselves to achieve pitch, yaw and roll control. Articulating the sail panels appeared more promising than vanes, because mechanical implementation was simpler there was less hardware to deploy and hence less mass and costs.

For the options involving shifting the center of mass relative to the center of pressure, we focused on articulating the entire spacecraft bus relative to the sail subsystem in order to move the largest possible mass and maximize control authority.The options considered were translating the boom in the plane of the sail and also rotating the bus on a short boom extended for the plane of the sail.The latter option was preferred because it was viewed as having a simpler mechanical implementation and because torques to the sail

Table 3.8: Loss factor for specimens with cork dust agglomerate CD1

frequencies	loss factor
97.45649	0.0261575
265.64063	0.0090225
514.42505	0.005255
851.50928	0.0047375
1264.49036	0.004525

Table 3.9: Loss factor for specimens with cork dust agglomerate CD2

frequencies	loss factor
119.57787	0.0186925
321.54361	0.0084
634.46667	0.0071225
1478.48865	0.00767
1536.49634	0.0678

subsystem could be minimized, presenting a more stable dynamic environment for the sail.

Ultimately, we select the boom articulation on a boom rather than articulating the sail panels because it minimized the complexity of the sail subsystem, and it also provided an implementation that could be readily adapted to many different sail designs, including spinning sails.The bus rotation is effected via rotation wheels minimizing the disturbance input to the sails subsystem dynamics. Once the bus is rotated to the desired control position, the bus is locked with a mechanical clutch to hold position. Sail rotation control is achieved via the reaction wheels with the chemical thrusters to unload the wheels.

The loads are going to study the compressive loads and lateral loads being these last of great importance because they can cause undesirable and fatal rupture of the Mylar sail that would end the mission. Orbital maneuvers which abut submitted this type of spacial ships are long periods of time, continuous low-thrust maneuvers due to the type of propulsion. By doing the AOCS to modify the path is assumed that there is a side load on the boom for a very small period of time, that is loaded as a model the lateral impulse at the end of the boom so as to produce the maximum displacement

Table 3.10: Loss factor for specimens with cork dust agglomerate CD3

frequencies	loss factor
101.35963	0.0231425
275.31253	0.00834
530.53149	0.0060275
866.54492	0.00598
1290.47144	0.0054

Figure 3.5: Test equipment

and thus get a better sense of the effects on the structure.

Load value is set at 1 N value slightly larger than usual in the space field, but serves to accentuate the possible effects the damping introduced in the boom.

The case of the boundary conditions impose that one end is fixed for a more realistic model possible.

3.5 Spatial discretization of the models

Because the computing power of computers growing every day and currently a workstation allows low cost make numerical calculations unthinkable years ago, the numerical simulation is increasingly important. Numerical simulation is now a design tool that allows to evaluate prototypes without the need for expensive experimental evidence in problems that are sufficiently validated mathematical models and can be used to determine the real-time behaviour of a simulated system.

The purpose of discretizing the continuous problem is reduced to a discrete solution for using the computer. The basic approach is to replace the

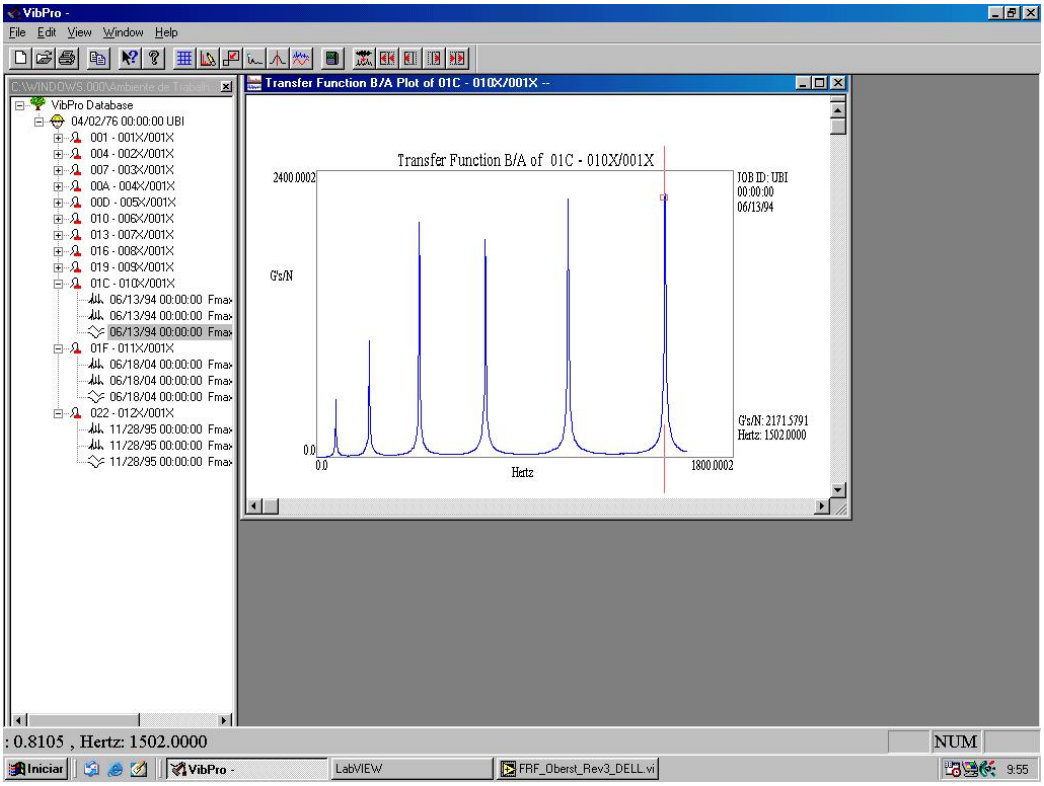

Figure 3.6: Vibpro Software

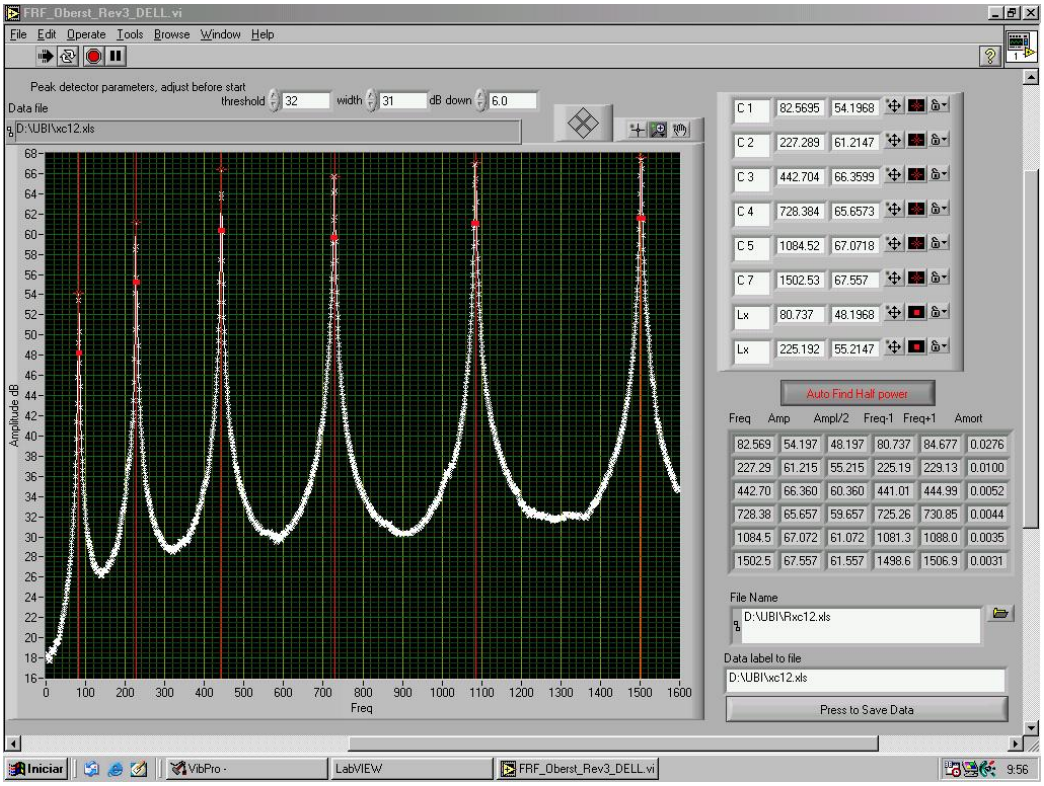

Figure 3.7: LabView Software

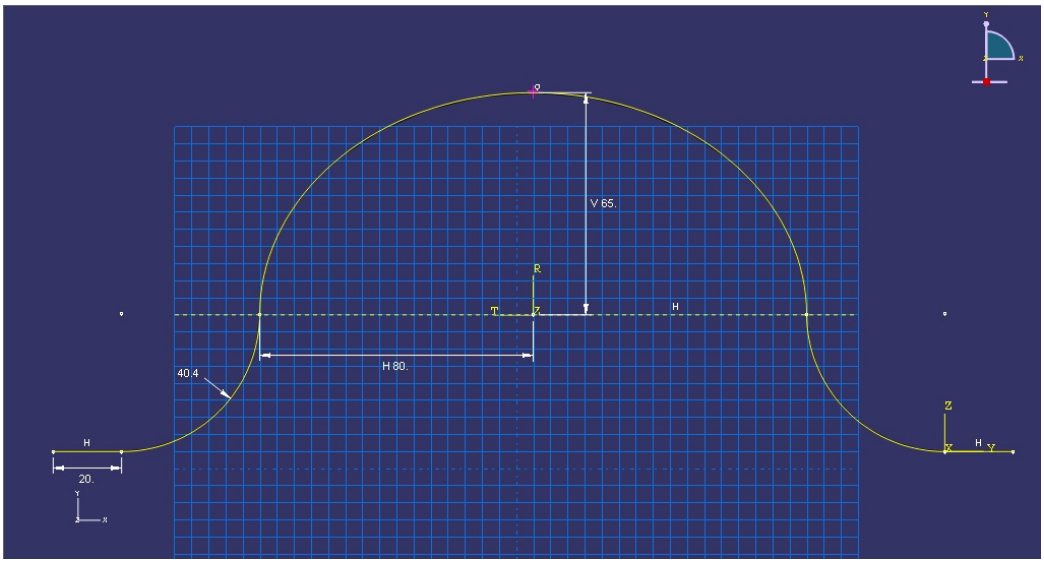

Figure 3.8: Boom section used in ABAQUS

continuous domain of integration by a mesh of discrete points that divide this into small sub-domains. Instead of developing a solution defined at any point in the domain, we obtain approximations for isolated points. Intermediate values between different discrete points, derivatives and integrals and other operators can be obtained from the discrete solution by interpolation techniques

3.6 Mesh

In this project we used a structured mesh. Is a non-uniform curvilinear grid, by an equation of transformation can be converted to a rectangular Cartesian mesh. Intersection of the coordinate lines are the nodes of the mesh. A structured mesh is defined when the appropriate position (x, y, z) of its nodes in a Cartesian axis. For each grid node coordinates spend three lines that allow us to reach our neighbouring nodes integration domain. The topology of a structured mesh in a 3D domain is well defined by three data structures of three indices that hold the position of the nodes x_{ijk} y_{ijk} z_{ijk} Although this type of mesh has some disadvantages such as problems in areas where the solution has abrupt changes, if we use a larger number of discrete points in these areas or on the contour to adapt the grid we obtain a mesh suitable for the type of geometry of the boom, relatively simple. To achieve

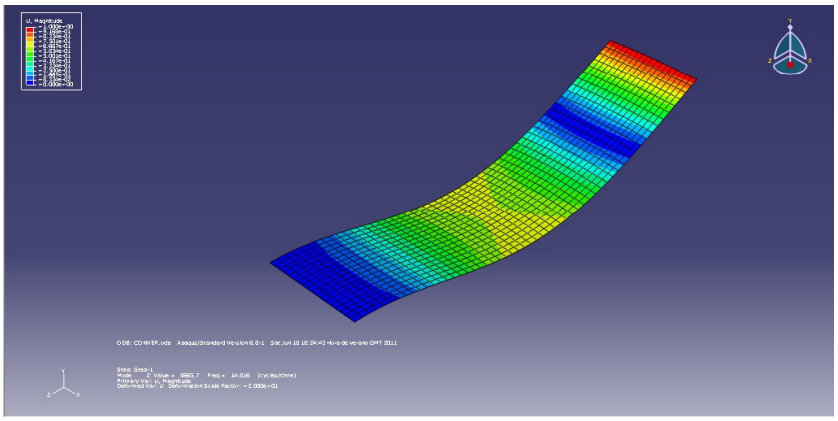

Figure 3.9: Mesh plate detail

maximum efficiency of our work, we analyzed mesh having as variable as the solution to obtain the natural frequencies of ABAQUS compared with a initial with a few elements to reach a compromise between precision and computational cost.

In the case of the plate we use a mesh of 990 elements. The analysis is shown in Table 3.11. The difference in the results of the last two meshes is considered small enough for the purposes of this work, while not involving excessively high computational cost. For a better understanding is an image 3.9 of the mesh for the second mode of the plate in bending.

The the boom model use a mesh of 30000 elements as is shown in Table 3.12.

3.7 Comparison and calibration ABAQUS results with other software

Is appropriate and necessary when we use any software, calibrate the results with a real model or in the worst known cases with the results of other software of the same kind.In this project we used the software ESAComp to perform a calibration before the simulations, to ensure that we successfully modelled a CFRP laminate structure in ABAQUS. ESAComp is software for analysis and design of composites initiated by the European Space Agency.

The plate considered is made of CFRP T300 and has a dimension 100 mm x 100 mm and a thickness of 2.4 mm embedded in one extreme and subjected to a load of 0.05 kN in the other. The stacking sequence is the following $[(45\ -45\ 0)_s]_2$. The maximum static displacement in the loaded extreme is 1.92 mm as appear in the figure 3.10. The result of ABAQUS is 1.924 mm. 3.11 So

Table 3.11: Mesh convergence study of the plate model

Number of elements	Result	Difference
10	23.5496	-
32	23.9278	0.3782
60	23.9121	0.0157
112	23.8619	0.0502
216	23.8421	0.0198
264	23.8258	0.0163
480	23.813	0.0128
560	23.8078	0.0052
640	23.8044	0.0034
800	23.8003	0.0041
990	23.7998	0.0005

Table 3.12: Mesh convergence study of the boom model

Number of elements	Result	Difference
15000	0.635127657	-
22500	0.635086547	0.0000411
30000	0.635073898	0.0000127

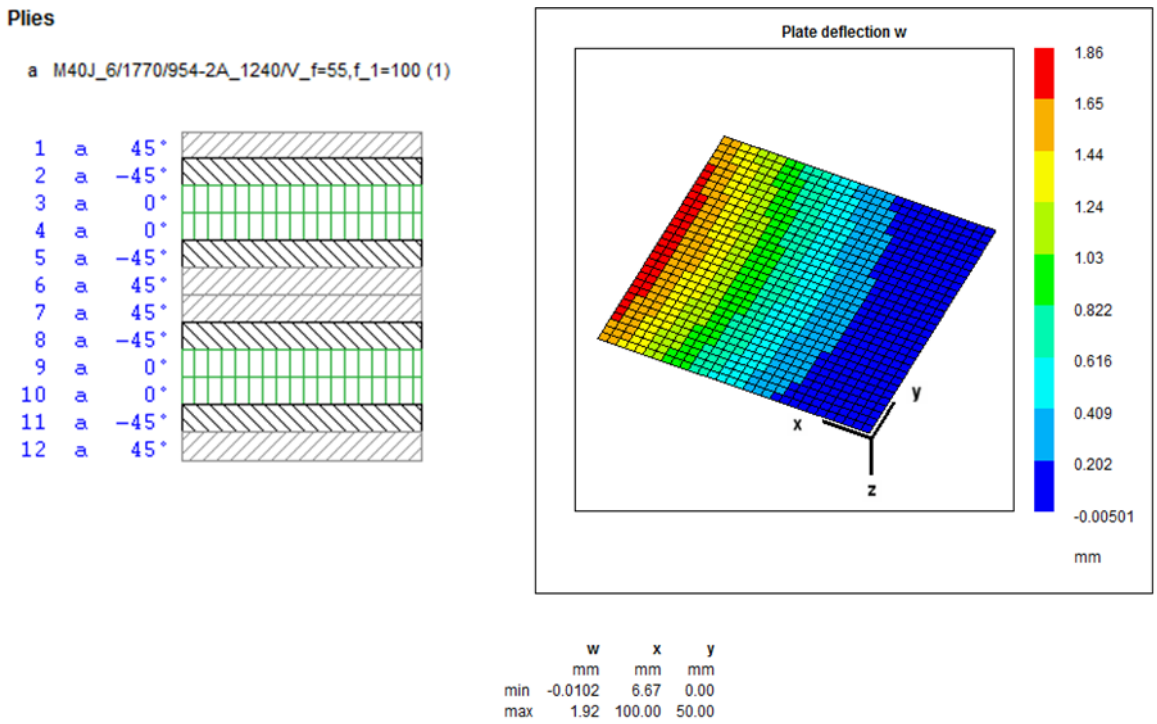

Figure 3.10: Esacomp results

we can conclude that the results of both programs coincide except minimal differences produced by a different mesh. Therefore, the composite model we introduced in ABAQUS is correct we can safely address the following simulations.

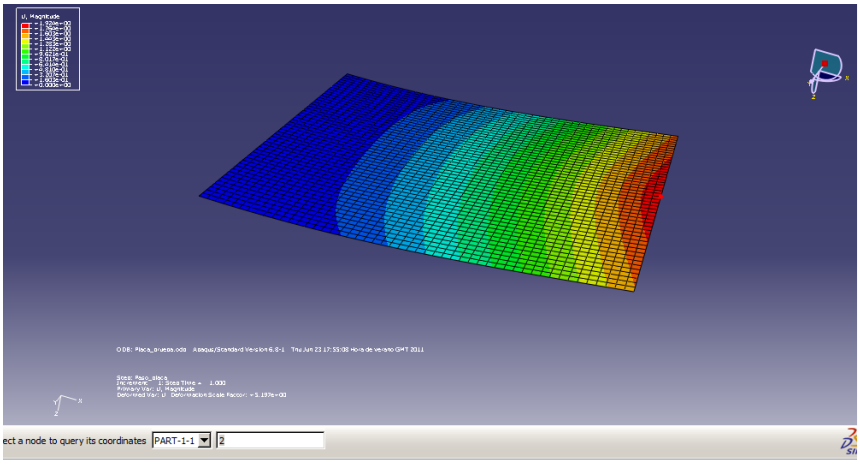

	1	2	3	Magnitude
	5.00000e+001,	0.00000e+000,	0.00000e+000,	–
	5.19701e+000,	5.19701e+000,	5.19701e+000,	–
led):	5.00000e+001,	−6.04459e−016,	−1.92418e+000,	–
i):	5.00000e+001,	−3.14138e−015,	−1.00000e+001,	–
	4.72366e−018,	−6.04459e−016,	−1.92418e+000,	1.92418e+000

Figure 3.11: ABAQUS results

Chapter 4

Results

4.1 Experimental results

First we will refer to laboratory tests.The results obtained after processing the data obtained is the test is represented graphically in the figure 3.1. In the graph we can see the value of loss factor for the three types of specimens tested. The frequency range is from 80 to 1500 Hz lower frequency is limited by the first mode of vibration of the plate to the test setup.It is important to say that the first mode Corresponding values can not be taken into account because both the precision of measuring instruments as the standard.

For a better interpretation of the results have been provided all the values of each specimen on the same graph so that they can observe the differences between specimens of different types and also the dispersion of values in the different specimens of each type, simply be seen by observing the distances between the same points for a given frequency. It can be seen that the specimens difference between each type is very small which gives a margin of safety to the results.From these results we can obtain the coefficient α for the Rayleigh damping model for the CFRP. The result of the other samples is not used as a input in ABAQUS , but it is an estimate and helps to understand the effects of introducing a viscoelastic material such as cork in the structure , either in a sandwich structure or dust homogeneously distributed.

4.2 Numerical results

We performed numerical simulation of two different specimens. First the specimen made for laboratory tests and secondly the new specimen with appropriate geometry for better visualization of final results. In the first case

shown in the graph are small perturbations along the time history of displacement, which may be due to weak shock waves in layered heterogeneous material as indicated by Tsai and Vikas (2005) [38]. this effects are caused by geometric parameters such layer thickness and the distance of wave propagation or density of interfaces, also the smallest layer thickness laminates contain the highest frequency oscillations while the largest layer thickness laminates contain the lowest frequency oscillations so these instabilities are present in samples of low thickness. Although the reviews of the instabilities of this type is far from the ultimate objectives of the project, its introduction is suitable as well as the result of the dynamic response of the specimen.The results of the specimen made in the laboratory are shows in the fig. 4.1 For this was the design of another specimen for numerical analysis where we could better appreciate the response. This specimen has dimensions of 200 mm x 50 mm and a width of 2.4 mm in the case of damped model is added a layer of cork of 0.9 mm. The dynamic response of this specimen is show in the fig.4.2

It is observed that the response of the specimen that has the cork layer oscillations are also those discussed above and can also be concluded that this is an overdamped response. The next step was to simulate this probe taking into account the existence of resin inside the cork layer has cured and therefore provide rigidity, which has not been taken into account, this means that the relative volume is 3%, which is a conservative value, considering that the value of E for a typical epoxy resin is about 3 GPa then we can assume a E of 100 MPa for the layer of cork. This yields a response that might be closer than expected by the experience and observations in the laboratory. This yields a response that might be closer than expected by the experience and observations in the laboratory but by no means intended to be a conclusive result because it would be necessary to study the percentage of resin that has penetrated and cured the cork .

Reproduce testing laboratory in ABAQUS to validate them is very complicated at the same time loses some of its practical meaning to having to use experimental values in the software. Therefore only the natural frequencies are extracted and compared with those obtained in the laboratory.

4.2.1 Plate numerical and experimental frequencies

The frequencies that are captured in the laboratory tests are due to bending modes

As we can see in 4.2 there is not much difference between the results, particularly for the lowest frequencies, which we conclude that the numerical model is quite close to reality in the case of CFRP laminate. In the case of

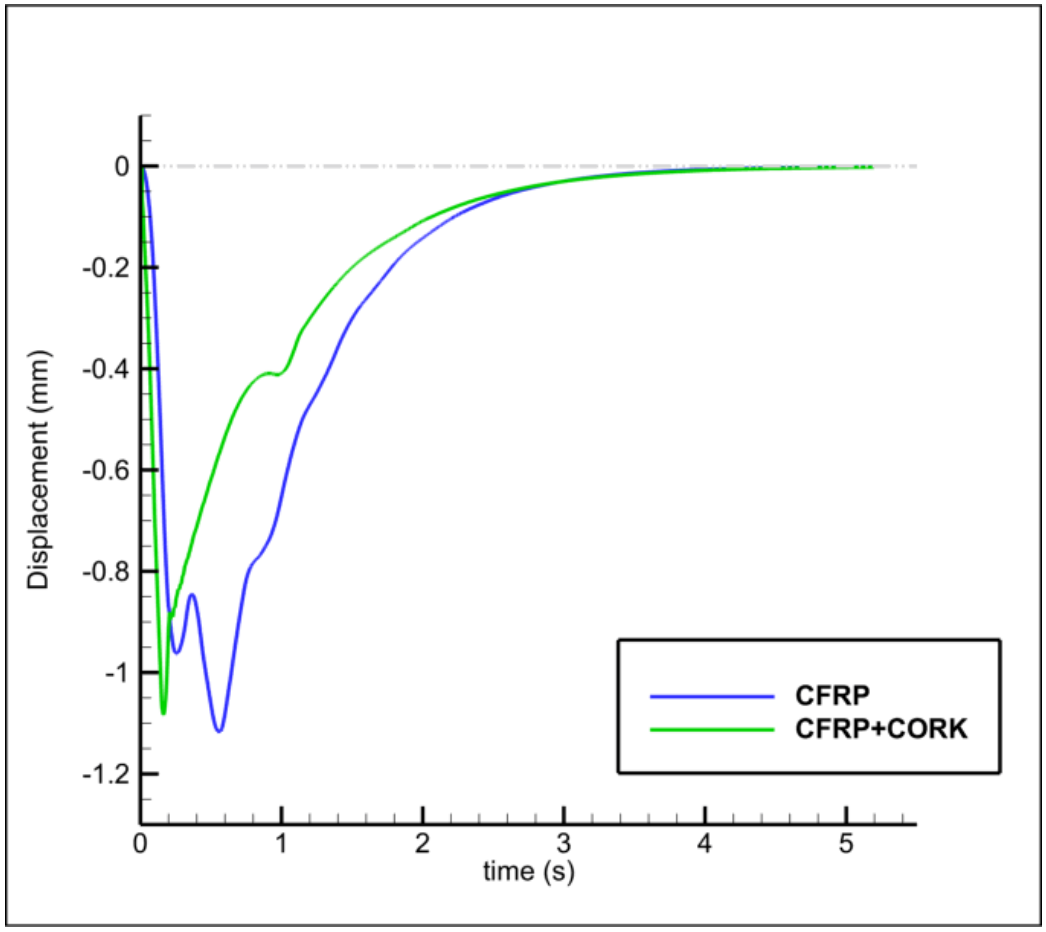

Figure 4.1: Dynamic response to an impulsive load for the original plate

Table 4.1: Comparison of five first eigenfrequencies for the specimen of laminated CFRP

Mode number	Experimental	Numeric
1	81.858	88.080
2	225.017	242.680
3	440.123	475.392
4	725.445	785.159
5	1079.527	1171.529

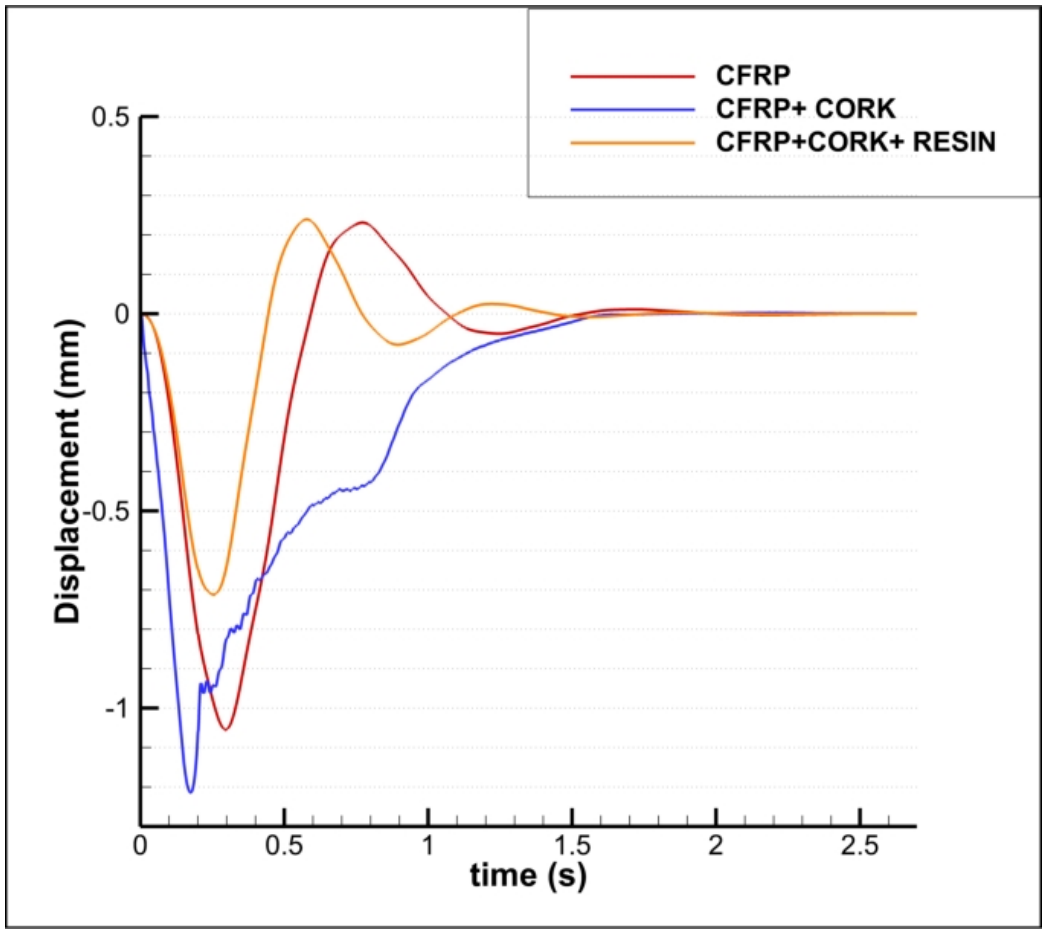

Figure 4.2: Dynamic response to an impulsive load for modified plate

Table 4.2: Five first eigenfrequencies detected in test for the specimen with a cork core

Mode number	Test
1	101.527
2	282.639
3	541.185
4	868.835
5	1250.836

cork core specimens proceeds in the same way except that in this case the natural frequencies of torsional and bending modes are very close together so even though it is expected that the excited modes are flexural not have absolute certainty that this is so and we can not clearly identify them. We can only say with certainty that the frequency of the first Bending mode captured in the trial can be clearly identified with the second bending mode calculated ABAQUS which has an approximate value of 94 Hz.

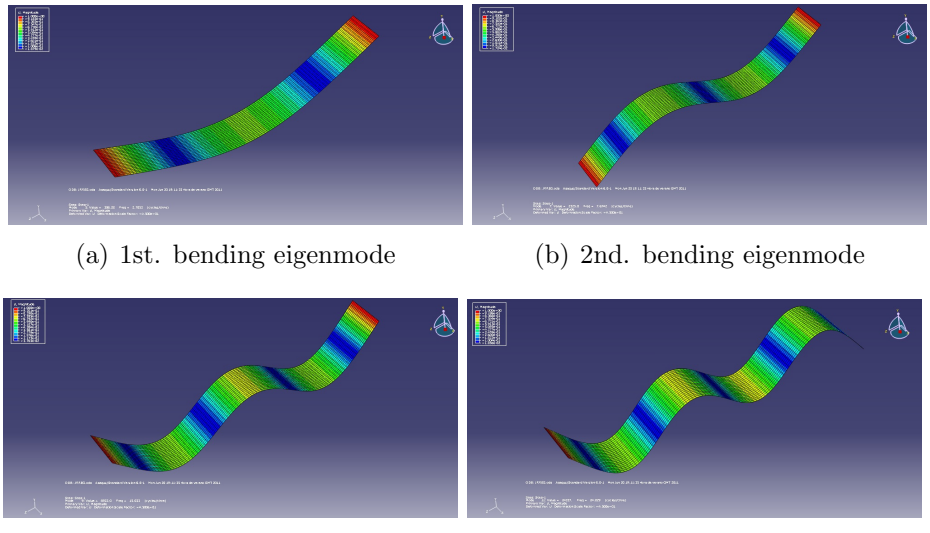

(a) 1st. bending eigenmode (b) 2nd. bending eigenmode

(c) 3rd. bendig eigenmode (d) 4th. bendig eigenmode

Figure 4.3: Eigenmodes in ABAQUS for the simple plate of CFRP

Table 4.3: Ten first eigenfrequencies for CFRP boom

Mode number	Frequency(Hz)
1	0.6351
2	0.8350
3	3.9765
4	5.2163
5	11.1156
6	14.3658
7	14.4163
8	14.5755
9	15.5705
10	18.3796

4.2.2 Boom dynamic analysis

Below are shown the first ten natural frequencies of CFRP boom and the boom modified with a layer of core cork, also we can see from the figures 4.4 and **??** the first four eigenmodes in both cases.

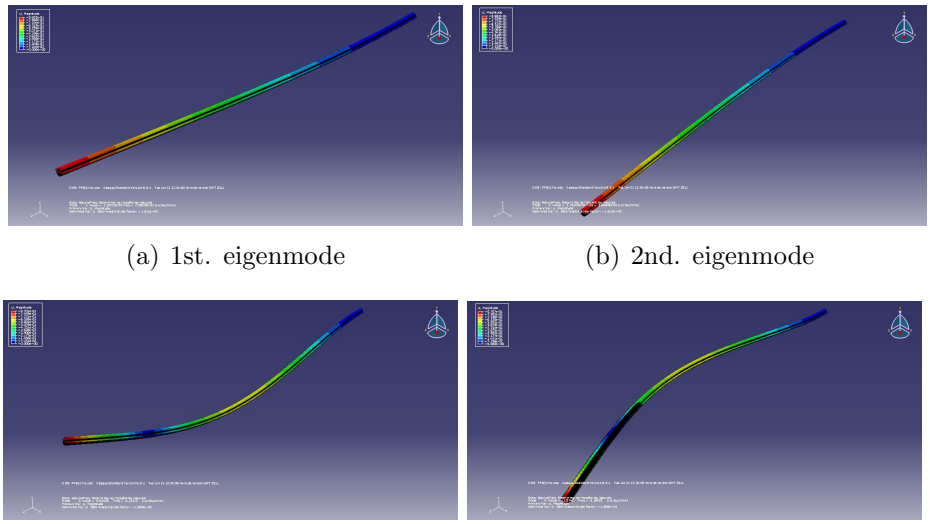

(a) 1st. eigenmode (b) 2nd. eigenmode

(c) 3rd. eigenmode (d) 4th. bendig eigenmode

Figure 4.4: Eigenmodes in ABAQUS for the simple CFRP boom

Table 4.4: Ten first eigenfrequencies for CFRP boom with core cork layer

Mode number	Frequency(Hz)
1	0.6299
2	0.8360
3	3.9445
4	5.2163
5	5.1826
6	11.0247
7	14.8327
8	14.8327
9	15.8368
10	18.5539

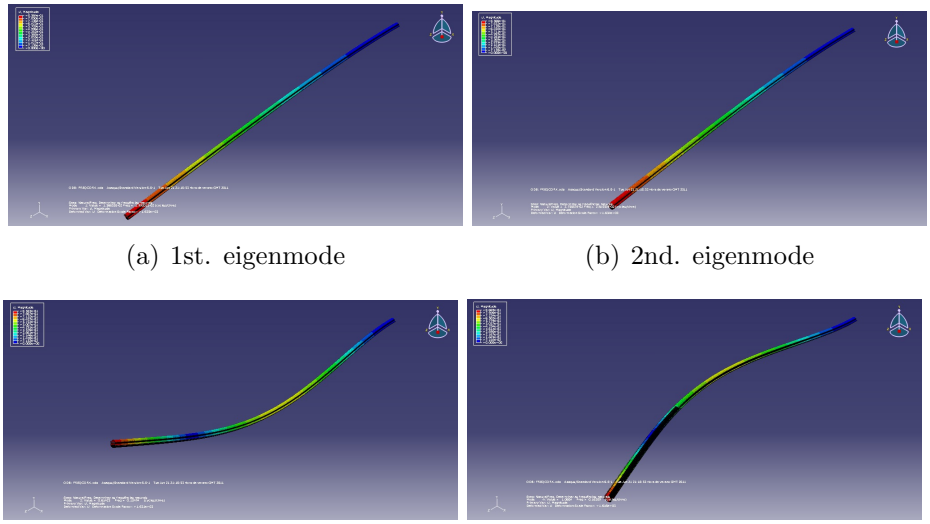

(a) 1st. eigenmode (b) 2nd. eigenmode

(c) 3rd. eigenmode (d) 4th. eigenmode

Figure 4.5: Eigenmodes in ABAQUS for the boom with core cork layer

Chapter 5

Conclusions

With the results of laboratory tests we obtain the following conclusions :

- For low frequencies the use of a of damping layer in a CFRP laminate structure of an increase of loss factor in the order 15% and this increase is very similar whether using a layer of dust agglomerate either in powder or sandwich.
- In the CFRP simple laminate, the laminate with a agglomerated cork dust layer and the laminate with a cork sandwich layer, loss factor decreases with increasing frequency.Loss factor decreases with increasing frequency to reach a value of about 500 Hz where the first and second mentioned configuration remains constant to 1300 Hz while for the third configuration, which uses the sandwich layer appears to have a slight increase with frequency.
- The increased value of the loss factor by using a layer of viscoelastic material is amplified by increasing the frequency value especially since the 400 hz or so to the configuration with a layer of agglomerate cork dust reaches increases until a 25% while for the cork sandwich layer configuration can reach 50% at 1300 Hz

With the results obtained in the FEA analysis obtained in the simulation with ABAQUS we get the following conclusions:

- Under the application of an impulsive load the use of a sandwich layer of cork in a laminated structure reduces the amplitude of the vibration produced,but this is only true for a given geometry, ie for a given geometry study is needed to check which is the best combination of the laminated layer of cork.

- The use of cork layer produces that the different eigenmodes are closer to each other. Causes torsion and bending modes are very close in a bandwidth relatively much lower than in the case without passive damping, this may be due to the decrease of stiffness in the section due to the introduction of a layer of core cork.

- In the case of the solar sail boom the use of a hypothetical layer of core cork, it can be seen that has not great influence on the natural frequencies of the original boom or even in the eigenmode associated with these frequencies.

Chapter 6

Future work and development

Due to time and resources have not been able to develop this project as much as possible. In general lines and further progress can be made on several fronts to improve the present from the experimental point of view to further improving implementation numerical model of viscoelastic material from the point of view in the field of computational optimization.

The two main improvements and enhancements include:

- Laboratory work and numerical implementation

  The logical step is to investigate the structural damping of the composite structure. Performing the test in the laboratory by the relevant tests. These results could model a more realistic dynamic response of a structure subjected to harmonic loads.

- Numerical Optimization

  Within the field of optimization the application of most interest and utility is the use of genetic algorithms (GA) for optimization of composite structures with and without layers of viscoelastic material. The optimization variables are generally geometric characteristics of the distribution of layers such as thickness and orientation. Optimization conditions vary depending on the objective to be optimized. As discussed above ([39]) the use of optimization in terms of the damping set a property of a layer of material has little interest, but it may be interesting from the standpoint of rigidity.

- Others: Study of instabilities in the dynamic response of laminated structures of low stiffness

References

[1] D.A. Saravanos and C.C. Chamis. Unified micromechanics of damping for unidirectional fiber reinforced composites. *NASA Technical Memorandum 102107*, 1989.

[2] D.A. Saravanos and C.C. Chamis. Mechanics of damping for fiber composite laminates including hygro-thermal effects. *NASA Technical Memorandum 102329*, 1989.

[3] M. Kaliske and H. Rothert. Damping characterization of unidirectional fibre reinforced polymer composites. *Composites Engineering*, 1995.

[4] C. Kyriazoglou and F.J. Guild. Finite element prediction of damping of composite gfrp and cfrp laminates a hybrid formulation vibration damping experiments and rayleigh damping. *Composites Science and Technology*, 2006.

[5] Daniel J. Inman. *Engineering Vibration*. Prentice Hall Internacional, Inc., 1994.

[6] R.M. Christensen. *Theory of viscoelasticity,an introduction. Second edition*. Academic press, 1982.

[7] John D. Ferry. *Viscoelastic properties of polymers*. Jonh Wiley & Sons, INC., 1980.

[8] T. Pritz. The poisson's loss factor of solid viscoelastic materials. *Journal of Sound and Vibration*, 2007.

[9] H. A. Waterman. Relations between loss angles in isotropic linear viscoelastic materials. *Rheol. Acta*, 1977.

[10] *Abaqus Analysis User's Manual. Vol I, II, III, IV*.

[11] *Structural Dynamics and Control of Large Space Structures.NASA Conference Publication 2187. NASA Langley Research Center.Hampton,Virginia*, 1980.

[12] D. Ungar, E.E.and Ross. Damping of flexural vibrations by alternate viscoelastic and elastic layers. *Proceedings of the Fourth Conference on Solid Mechanics. University of Texas, Austin,TX.*, 1959.

[13] B.I. Lazan, A.F. Metherell, and G. Sokol. Multiple-ban surface treatments for hight damping. *Technical report AFML-TR-65-269*, 1965.

[14] Jerome Ruzicka, E. Thomas, F. Derby, De W. Schubert, and Jerome S. Pepi. Damping of structural composites viscoelastic shear-damping mechanisms. *Nasa Contractor Report*, 1967.

[15] R. Plunkett and C. T. Lee. Length optimization for a constrained viscoelastic layer damping. *Technical Report AFML-TR-68-376*, 1972.

[16] Benjamin P. Dolgin. Composite passive damping struts for large precision structures. *United States Patent.Patent Number: 5,203,435*, 1993.

[17] A.L. Araújo, C.M. Mota Soares, C.A. Mota Soares, and J. Herskovitsc. Damping optimization of viscoelastic laminated sandwich composite structures. *EngOpt 2008-International Conference on Engineering Optimization Rio de Janeiro, Brazil*, 2008.

[18] Christoph Sickinger, Lars Herbeck, and Elmar Breitbach. Structural engineering on deployable cfrp booms for a solar propelled sailcraft. *Acta Astronautica*, 2005.

[19] Joachim Block, Marco Straubel, and Martin Wiedemann. Ultralight deployable booms for solar sails and other large gossamer structures in space. *Acta Astronautica*, 2010.

[20] Luis Gil. *Cortiça. Produção,tecnologia e aplicação.* Instituno Nacional de Engenharia e Tecnologia Industrial, 1998.

[21] João F. Mano. The viscoelastic properties of cork. *Journal of material Science*, 2002.

[22] Osvaldo Castro, José M. Silva, Tessaleno Devezas, Arlindo Silva, and Luís Gil. Cork agglomerates as an ideal core material in lightweight structures. *Materials and Design*, 2010.

[23] C.P. Gameiro and J. Cirne. Dynamic axial crushing of short to long circular aluminium tubes with agglomerate cork ller. *Mechanical Science*, 2007.

[24] Ronald F. Gibson. Modal vibration response measurements for characterization of composite materials and structures. *Composites Science and Technology*, 2000.

[25] Kyo-Nam Koo. Vibration and damping analysis of composite plates using finite elements with layerwise in-plane displacements. *Computers and Structures*, 2002.

[26] A.L. Araújo, P. Martins, C.M. Mota Soares, C.A. Mota Soares, and J. Herskovits. Damping optimisation of hybrid activepassive sandwich composite structures. *Advances in Engineering Software*, 2010.

[27] J. A. Güemes, P. Muñoz Esquer, and J.M. Menéndez. *Materiales Compuestos*. Publicaciones de la Escuela Técnica Superior de Ingenieros Aeronáutica, 2006.

[28] C. Martinez Arnaiz. *Cálculo estructural. Método de los elementos finitos*. Publicaciones de la Escuela Técnica Superior de Ingenieros Aeronáutica, 1998.

[29] J. A. Hernández and E. Valero. *Análisis y cáluculo numérico en ecuaciones en derivadas parciales*. Publicaciones de la Escuela Técnica Superior de Ingenieros Aeronáutica, 2002.

[30] Benjamin L. Diedrich. Attitude control and dynamics of solar sails. Master's thesis, University of Washington, 2001.

[31] Chi-Tsong Chen. *Linear system theory and design*. Oxford University Press, 1999.

[32] Katsuhiko Ogata. *System dynamics*. Prentice Hall, 1987.

[33] Williams W. Seto. *Vibraciones mecánicas*. McGraw-Hill, 1977.

[34] James Richard Wertz and Wiley J. Larson. *Space mission analysis and design*. Microcosm, 1999.

[35] Michal Rak and Mohamed Ichchou. Determination of loss factor for beams with viscoelastic layer by means of methods based on wave propagation. *II Eccomas Thematic Conference On Smart Structures And Materials*, 2005.

[36] *Abaqus/Standard User's Manual Vol. I, II, III.*

[37] *Abaqus Example Problems Manual. Vol. I and II.*

[38] Liren Tsai and Vikas Prakash. Structure of weak shock waves in 2-d layered material systems. *International Journal of Solids and Structures*, 2005.

[39] E.E. Ungar and D. Ross. Damping of flexural vibrations by alternate viscoelastic and elastic layers. *Proceedings of the Fourth Conference on Solid Mechanics*, 1959.